doi:10.1017/S1431927614011192
Microsc. Microanal. 20 (Suppl 3), 2014

Effect of Nitrogen Content on the Microstructure and Hardness of Hard Zr–B–C–N Films

Minghui Zhang[1], Jiechao Jiang[1], Jaroslav Vlček[2], Petr Steidl[2], Jiri Kohout, Radomir Cerstvy and Efstathios I. Meletis[1]

[1.] Department of Materials Science and Engineering, The University of Texas at Arlington, Arlington, Texas 76019, USA.
[2.] Department of Physics, University of West Bohemia, Univerzitní 22, 306 14 Plzeň, Czech Republic.

Nanostructured multicomponent films of transition metal-based carbonitrides quaternary were found to have a much wider industry-specific applications due to their outstanding properties compared to the traditional binary or ternary hard coatings [1, 2]. For example, the novel quaternary Si-B-C-N system exhibits an extraordinary high-temperature oxidation resistance and stability [3-5], while it maintains its amorphous structure at high temperatures [6]. Recently, multifunctional Zr-B-C-N films have been fabricated by pulsed reactive magnetron sputtering that can be used as hard protective coatings with high oxidation and corrosion resistance at elevated temperatures [7]. These are high-quality, defect-free films with smooth surfaces (average roughness $R_a \leq 4$ nm) and good adhesion to substrates.

In this work, we have employed high-resolution transmission electron microscopy, electron diffraction, X-ray photoelectron spectroscopy and nano indentation to systematically study the microstructures and mechanical properties of Zr-B-C-N films. Four films with a chemical composition of $Zr_{61}B_{27}C_6N_3$, $Zr_{41}B_{30}C_8N_{20}$, $Zr_{26}B_{26}C_6N_{42}$ and $Zr_{24}B_{19}C_6N_{49}$ were deposited on p-type Si (100) by pulsed reactive magnetron sputtering of Zr, B, and C from a single B_4C–Zr target in the nitrogen-argon gas mixtures with a nitrogen fraction of 0%, 5%, 10% and 15%. The B_4C–Zr target was prepared using a B_4C plate overlapped by Zr stripes covering 45% in the target erosion area. During the deposition, the substrate temperature was adjusted to 450 °C by an infrared heater on the substrates at a floating potential. The base pressure was 3×10^{-3} Pa and the total pressure of argon–nitrogen gas mixtures was 0.5 Pa.

The $Zr_{61}B_{27}C_6N_3$ film is a composite material involving an amorphous structure surrounding face-centered cubic (fcc) B-rich Zr(B,C,N) nano-columnar structures in which the B-rich Zr(B,C,N) crystalline has a [111] preferred orientation (Fig. 1(a)). The $Zr_{41}B_{30}C_8N_{20}$ film consists of nano-needle structures which have a length of about 40 nm and a width of about10 nm (Fig. 1(b)). This film was found to possess the highest hardness (36.4 GPa) and modulus (316.8 GPa). The nano-needles have a fcc structure and are composed of ZrN and/or Zr(B,N) nano-domain structures (~2 nm) that are semi-coherently joined by ZrN monolayer interfaces (Fig. 2). The $Zr_{26}B_{26}C_6N_{42}$ film deposited with 10% N2 fraction in the gas mixture is composed of refined crystalline ZrN nano-needle structures (~2 nm) embedded in an amorphous matrix (Fig. 1(c)). The $Zr_{24}B_{19}C_6N_{49}$ film has a pure amorphous-like structure (Fig. 1(d)). These results helped us to develop a better understanding of the relationship between the microstructure and the mechanical properties of the Zr-B-C-N films. The highest hardness obtained for the $Zr_{41}B_{30}C_8N_{20}$ film is attributed to the particular microstructure that involves Hall-Petch strengthening effects from the ZrN and/or Zr(B,N) nanograins, and interface layer strengthening from the semi-coherent Zr-N monolayer boundary. The results showed that an amorphous structure can be introduced into the films by changing the N/Zr ratio via varying the N_2 fraction in the N_2/Ar gas mixture. Formation of such an amorphous structure has a negative impact on the mechanical properties of the films.

References:

[1] M. Braic, M. Balacenu, A. Vladescu, C.N. Zoita and V. Braic, Thin Solid Films **519** (2011) 4092.
[2] Y.H. Cheng, T. Browne, B. Heckerman and E.I. Meletis, Surf. Coat. Technol., **205** (2011)4024.
[3] J. Vlček *et al,* J. Vac. Sci. Technol., **A 26** (2008) 1101.
[4] J. Čapek, *et al,* Surf. Coat. Technol. , **203** (2008) 466.
[5] J. Houška, J. Vlček, Š. Potocký, V. Peřina, Diamond Relat. Mater., **16** (2007) 29.
[6] J. He *et al,* Thin Solid Films, **542** (2013)167.
[7] J. Vlček *et al,* Surf. Coat. Technol., **215** (2013) 186.
[8] This work was supported by the National Science Foundation under Award NSF/CMMI 1335502.

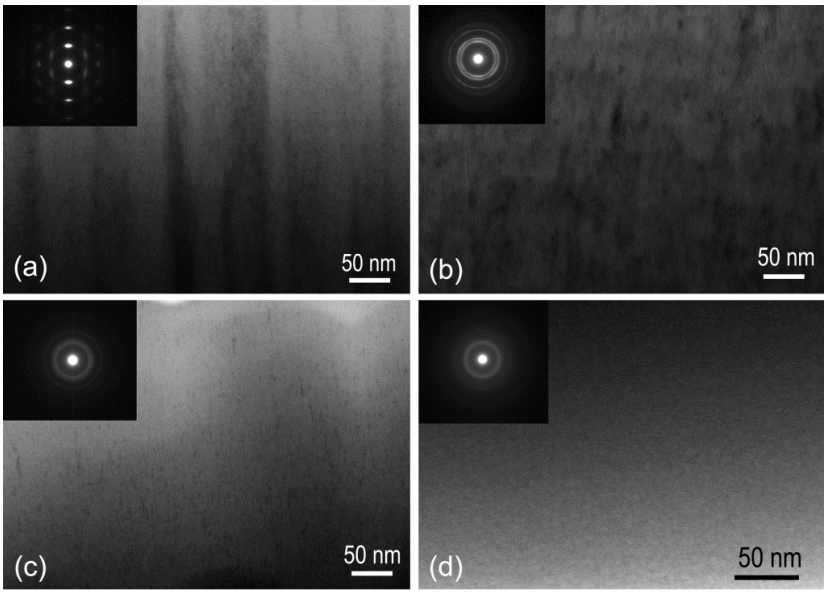

Figure 1. Cross-section TEM image and SAED pattern (inset) of the film (a) $Zr_{61}B_{27}C_6N_3$, (b) $Zr_{41}B_{30}C_8N_{20}$, (c) $Zr_{26}B_{26}C_6N_{42}$ and (d)$Zr_{24}B_{19}C_6N_{49}$.

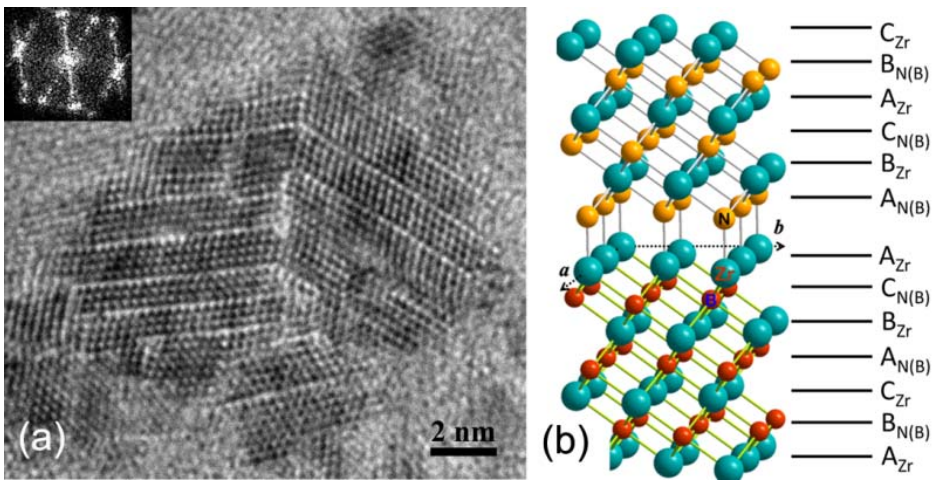

Figure 2. (a) HRTEM image of a nano needle in the $Zr_{41}B_{30}C_8N_{20}$ film showing nano domains separated by monolayer interfaces; (b) schematic illustration of atomic structure of the monolayer interface.

https://doi.org/10.1017/S1431927614011192 Published online by Cambridge University Press